This is a self-archived version of an original article. This version may differ from the original in pagination and typographic details.

Author(s): Trops, Roberts; Hakola, Anna-Maria; Jääskeläinen, Severi; Näsilä, Antti; Annala, Leevi; Eskelinen, Matti; Saari, Heikki; Pölönen, Ilkka; Rissanen, Anna

Title: Miniature MOEMS hyperspectral imager with versatile analysis tools

Year: 2019

Version: Accepted version (Final draft)

Copyright: © 2019 Society of Photo-Optical Instrumentation Engineers (SPIE).

Rights: In Copyright

Rights url: http://rightsstatements.org/page/InC/1.0/?language=en

Please cite the original version:

Trops, R., Hakola, A.-M., Jääskeläinen, S., Näsilä, A., Annala, L., Eskelinen, M., Saari, H., Pölönen, I., & Rissanen, A. (2019). Miniature MOEMS hyperspectral imager with versatile analysis tools. In W. Piyawattanametha, Y.-H. Park, & H. Zappe (Eds.), Proceedings of SPIE Volume 10931 : MOEMS and Miniaturized Systems XVIII; 109310W (Article 109310W). SPIE, The International Society for Optical Engineering. SPIE conference proceedings, 10931. https://doi.org/10.1117/12.2506366

Miniature MOEMS hyperspectral imager with versatile analysis tools

Roberts Trops[a], Anna-Maria Hakola[b], Severi Jääskeläinen[b], Antti Näsilä[a], Leevi Annala[b], Matti A. Eskelinen[b], Heikki Saari[a], Ilkka Pölönen[b], and Anna Rissanen*[a]

[a]VTT Technical Research Centre of Finland, Espoo, Finland
[b]Faculty of Information Technology, Jyväskylä University, Jyväskylä, Finland

ABSTRACT

The Fabry-Perot interferometers (FPI) are essential components of many hyperspectral imagers (HSI). While the Piezo-FPI (PFPI) are still very relevant in low volume, high performance applications, the tunable MOEMS FPI (MFPI) technology enables volume-scalable manufacturing, thus having potential to be a major game changer with the advantages of low costs and miniaturization. However, before a FPI can be utilized, it must be integrated with matching optical assembly, driving electronics and imaging sensor. Most importantly, the whole HSI system must be calibrated to account for wide variety of unwanted physical and environmental effects, that significantly influence quality of hyperspectral data. Another challenge of hyperspectral imaging is the applicability of produced raw data. Typically it is relatively low and an application specific software is necessary to turn data into meaningful information. A versatile analysis tools can help to breach the gap between raw hyperspectral data and the user application. This paper presents a novel HSI hardware platform that is compatible with both MFPI and PFPI technologies. With an MFPI installed, the new imager can have operating range of $\lambda = 600 - 1000$ nm with FWHM of $15 - 25$ nm and tuning speed of < 2 ms. Similar to previous imager in Ref. 1, the new integrated HSI system is well suited for mobile and cloud based applications due to its small dimensions and connectivity options. In addition to new hardware platform, a new hyperspectral imaging analysis software was developed. The new software used in conjunction with the HSI provides a platform for spectral data acquisition and a versatile analysis tool for a processing raw data into more meaningful information.

Keywords: Fabry-Perot interferometer, hyperspectral imager, MOEMS, VNIR, data analysis

1. INTRODUCTION

The advances in Fabry-Perot (FPI) interferometer technology has led the development of new miniaturized micro-spectrometers. These micro-spectrometers can be integrated in portable mobile devices, such as smartphones and tablets as well as specialized industrial equipment. The possibility to non-intrusively analyze spectral information of objects with mass producible mobile hyperspectral device is something that has applications in many different areas, such as agriculture, medicine, remote sensing and waste recycling.

The typical way of developing FPI based spectrometers involves selection FPI that offers best performance for the particular use case. The mechanics, optics and electronics are designed to adapt to selected FPI and imaging sensor. Unlike the previous imagers the new hardware described in this paper can be configured by interchanging FPIs and optics. With this feature, the capabilities of HSI hardware are extended and the same hardware platform can be used in more applications. Another challenge of hyperspectral imaging is the analysis of hyperspectral data cubes. The hyperspectral data cube contains the information about reflectance of light in certain wavelength range, yet unique spectral features might not be immediately apparent to the user. Each pixel in image has its own spectral response, but it is difficult to visualize and perceive such large amounts of data at once. In addition the spectra of each pixel might not even be relevant in most cases. Instead the user is typically interested in abundance or just existence of certain unique spectral features and the spatial information. This makes use of microspectrometers more challenging. It is not clear if the raw hyperspectral data contain

Further author information: (Send correspondence to Roberts Trops*)
Roberts Trops: E-mail: roberts.trops@vtt.fi, Telephone: +358-4017-6004-9, www.vtt.fi

any meaningful information. Furthermore, if there are any unique spectral features it is important to visualize in which ares of image these features occur.

Overall, it is clear that the emerging technologies for microspectrometers require a versatile and low cost hardware development platform as well as a data analysis tool, that would help the user to easily extract the most significant information out of hyperspectral data.

2. FABRY-PEROT INTERFEROMETER

Fabry-Perot interferometer is a type of optical measurement device, that utilizes two parallel mirrors to produce certain spectral response. There two main types of FPIs that VTT is developing. These types are MOEMS FPI (MFPI) and Piezo-actuated FPI (PFPI) both of which posses different inherent advantages, when used in hyperspectral imaging applications. Both types are electrically tunable, yet each of them employ a different actuation method. Typically the selection of FPI type for HSI is based on their general features. These features are summarized in table 1 and described in Ref. 2. Overall, the PFPIs with larger optical apertures are better for high performance applications where high signal-to-noise ratio (SNR) is essential. In contrast, MFPIs are excellent for volume scaling and applications where low sensor cost is necessary.

Table 1: General features of MFPI and PFPI technologies.

Technology	PFPI	MFPI
Manufacturing	Assembled structure for small-to-medium volumes	Mass-producible wafer-level processes scalable to volume manufacturing
Optical apertures	Up to 24 (mm) allow high throughput of light	Optical apertures of 2–4 (mm)
Passband tuning	Wide tuning range and easy mirror customization	Tuning range determined by mirrors

The MEMS FPI has a near-zero loss quartz substrate for visible range (wavelengths approximately $400 - 800$ nm). The figure 1 shows the structure of an MFPI chip. A drive voltage is applied to electrodes of MFPI to change the passband. If the drive voltage is exceeded, the mirrors in MFPI are pulled together by attractive electrostatic force created by the electric field between mirrors. This is called pull-in and it is typically non-reversible or not easily reversible state, depending on the conditions the pull-in occurred. Even chips that are manufactured on the same wafer will likely have different maximum drive voltage values. For practical purposes pull-in means that for the MFPI can no longer be used. This is typically avoided by charecterizing MFPI chips and settings hardware or software limits on voltage applied to the MFPI.[3]

Unlike the PFPIs the MFPIs can be mass-produced by using modern semiconductor fabrication techniques. This allows the chips to be made at much lower price. The MFPI chips are first manufactured on wafers, then diced and finally packaged. Figure 2 shows diced MFPI chips in a tray and a single packaged PFPI. The packaging adds mechanical protection, electrical interface and additional circuitry for FPIs.
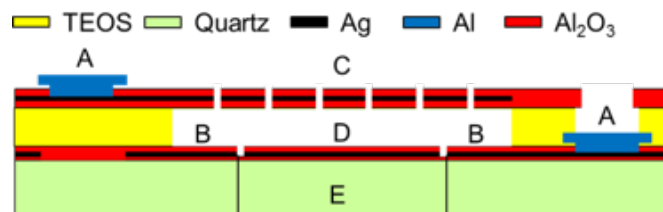

Figure 1: Structure of the MFPI. A: Contact pads; B: Actuation electrode; C: Upper movable mirror; D: Lower fixed mirror; E: Optical aperture.[1]

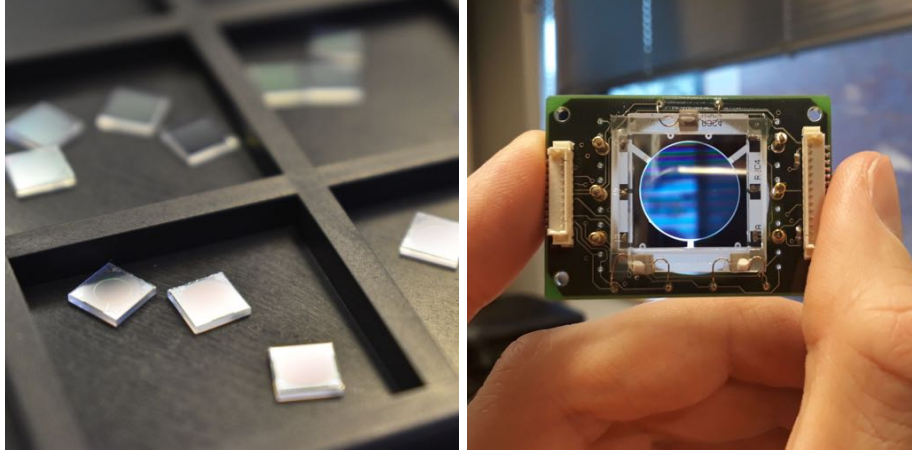Figure 2: Unpackaged 5x5 mm MFPI chips (left) and packaged PFPI (right).

3. HYPERSPECTRAL IMAGER CONCEPT

This section describes a hyperspectral imaging hardware platform, that was developed based on MFPI and PFPI technologies. This platform is developed to be pseudo-autonomous system, that has integrated embedded Linux computer, that handles data acquisition, pre-processing, storage and transferring of data. In addition, the Linux computer has Ethernet, USB and WiFi connectivity, which can be used to add additional instruments or transfer image data. In addition to interchangeable FPIs, the hardware allows different optical assemblies.

3.1 Electronics

The new hyperspectral imager electronics design is partly based on previous hand-held imager design described in Ref. 1. The main components are camera module, which has MT9P031 5MP 12-bit CMOS sensor, Linux embedded computer and FPI controller. The camera module is connected to Linux computer via USB. The images are acquired using Python API. Similar to previous camera, the new design uses a controller board to interface between processing unit and respective FPI installed in imager.

3.2 Mechanics and optics

The optomechanical part of imager seen in figure 3 consists of aluminum baseplate, that holds optics, MFPI and sensor. In addition, it provides a way to focus and adapt the optics for different applications. The 3D printed case of imager can be seen in 4. It was designed to allow easy access to optomechanics, enclose electronics and provide tripod mounting interface. The table 2 summarizes two different PFPI and MFPI configurations, which the new HSI concept supports. These parameters are the most commonly used to describe FPIs, as well as select them for certain application, therefore having a hardware platform that is compatible with both types is a major advantage.

3.3 System calibration

After assembling HSI, it is necessary to perform system calibration. The monochromator setup shown in figure 5 is used to measure and calculate the spectral response of each pixel in camera sensor by gradually changing the wavelength of monochromatic light and the passband of FPI. Light from halogen lamp is passed into monochromator. Then, monochromatic light is passed into a integrating sphere, which has a reference detector and HSI attached. The passband of FPI and monochromator output are changed by software script running on PC. In addition, PC captures the images and calculates values for calibration table.

Table 2: Hardware configurations of HSI.

FPI type	$PFPI$	$MFPI$
Spectral range (nm)	$450 - 850$	$600 - 1000$
Spectral resolution (nm)	$7 - 25$ @ FWHM	$15 - 25$ @ FWHM
Settling time* (ms)	10	2
Clear aperture (mm)	14	2.5

*Settling time for small wavelength steps (typ. <10 nm).

3.4 Measurement calibration

In order to capture a valid hyperspectral data cube, first it is necessary to perform measurement calibration sequence. The calibration sequence consists of capturing the dark reference and a white reference. Measurement calibration has to be repeated in case of changes in the light source or significant changes in the temperature of imaging sensor and FPI. White reference target is typically a diffused target, that has uniformly high reflectance over whole measured wavelength range. The dark reference target is typically a highly absorbing material, that is used to fully cover the aperture of imager, while dark signal level is recorded.

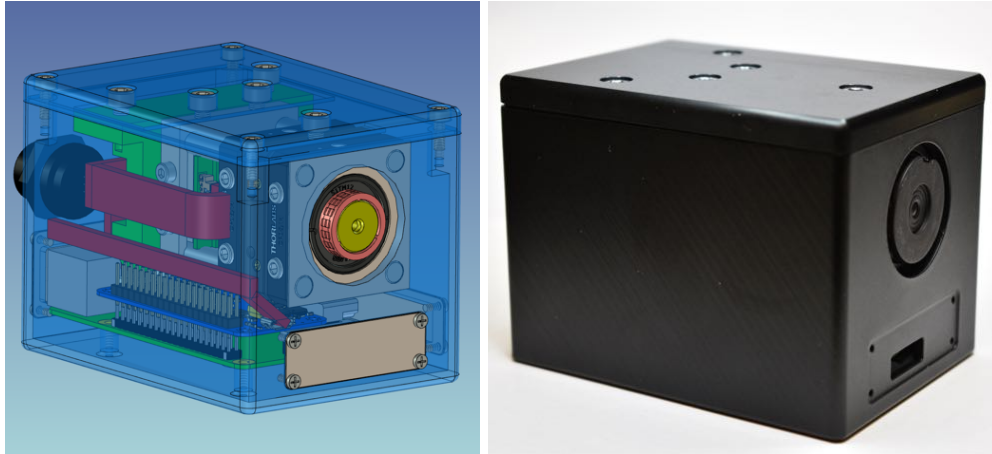Figure 3: Interchangeable optomechanics mounted to baseplate.

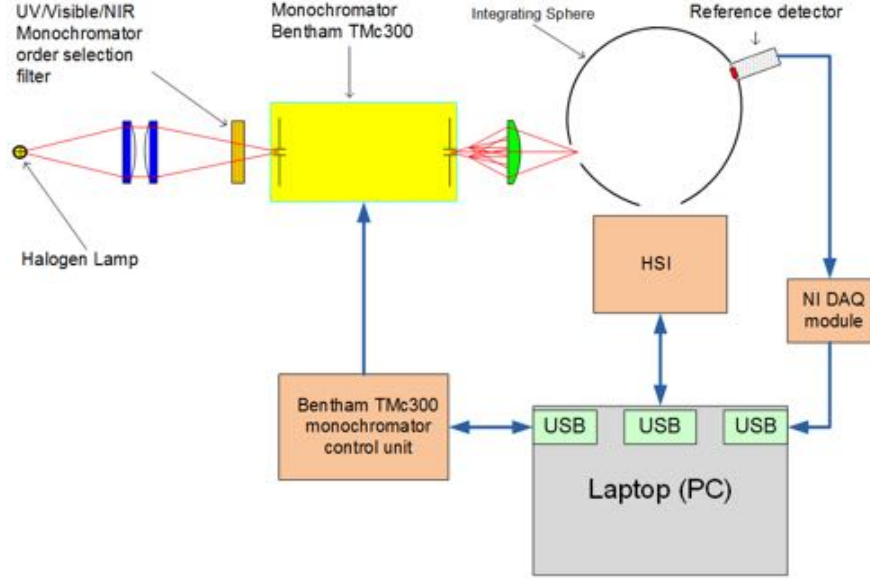Figure 4: 3D CAD model and assembled version of hyperspectral imager.

Figure 5: Monochromator calibration setup for HSI.

4. CUBEVIEW SOFTWARE

CubeView is a software, created by the Spectral Imaging Laboratory from the University of Jyväskylä, Finland. It's main purpose is to offer an easy to use and simple, but scientifically accurate interface for spectral imaging and spectral analysis. Software will be released under MIT license and one of the main strengths compared to other similar softwares is the compatibility with GeniCam standard. Other worth to mention features are the different ways to use CubeView: with devices it provides easy and fast imaging and without devices it can be used for analyzing an existing spectral data cubes.

4.1 Functionality

The essence of CubeView is the deep understanding of user requests and needs by using design thinking methods through the development phases. User requests and needs were based on Spectral Imaging Laboratory's past and ongoing research. The core of CubeView uses Spectral Imaging Laboratory's python libraries, `fpipy`,[4] `pyspindl`[5] and `spectracular`. CubeView has three main functionalities: LiveView, CubeView (imager) and CubeView Analyze.

LiveView is part of LiveView imager and it's main function is to offer video stream from the hyperspectral camera. LiveView has camera settings tool (based on `spectracular`), and some helpful functionalities to adjust imaging session settings. CubeView uses mainly `fpipy` and provides the view over captured cubes. Users can easily slide through raw, reflectance or radiance cubes, check radiance pixel spectra, or select frames by wavelengths to closer attention. CubeView uses `matplotlib` back-end with visualizations and saves and reads data from netCDF format.

CubeView Analyze analysis tool is created so that users can customize it according to their wishes and needs. Selected algorithms, including spectral unmixing based on vertex component analysis and fast least-squares approach, spectral angle mapper, principal component analysis and library of spectral indices are integrated to the basic version of CubeView Analyze. Users own analysis algorithms are easy to add to tool.

4.2 Algorithm

In spectral unmixing we assume that spectra are a linear mixture of some spectra, which are characteristic to the image and present in it. Now, let X be list of imaged spectra. Then linear mixture can be expressed in

matrix form following way

$$X = YM, \tag{1}$$

where $M \subset R^{k \times n}$ is the mixing matrix and $Y \subset R^{d \times k}$ are characteristic spectra, which are called endmembers. Here n is number of spectra in image, d is number of spectral bands and k is number endmembers. To solve M from the equation it is necessary to determinate the endmembers Y.

There are different ways to approach to determinate Y from the imaged data. If we rely on data's geometry, we can project data to the low dimensional space and try to determinate convex hull, which is covering all or majority of data points. Now, vertices of this hull are considered as endmembers. There are several methods, which are developed to detect these vertices, such as the vertex component analysis (VCA)[6] or Pixel-Purity Index (PPI).[7] Our implemented unmixing method uses VCA to determinate endmembers.

As evident there are several ways to determinate M after endmember detection. If we discard some boundary conditions, most easiest way to solve M is to use least-square method with pseudoinversion.[8] It holds that

$$\left(Y^T Y\right)^{-1} Y^T X = M. \tag{2}$$

This quite simple matrix operation solves M for us.

Spectral angle mapper is relatively simple measurement to compare similarity of two spectra.[9] We measure angle between spectra $\mathbf{x}$ and $\mathbf{y}$ by calculating angle between these two vectors. Spectral angle

$$\theta = cos^{-1} \frac{\mathbf{x} \cdot \mathbf{y}}{\|\mathbf{x}\| \cdot \|\mathbf{y}\|}, \tag{3}$$

where $\|,\|$ is euclidean norm of the vector. By selecting some threshold for the angle θ is SAM actually a binary classificator. In analysis example user has to select reference spectra from the spectral image.

With principal component analysis (PCA) it is possible to search those components which are causing most of the variance within recorded spectra. The difference between PCA and spectral unmixing is that PCA doesn't take account any physical meaning. Thus we will just see which areas of the image is causing variance, while spectral unmixing can actually tell us, which spectra's are present in the data cube. PCA's implementation is straight forward. First, we center data around origo by extracting mean of each spectra. Then we calculate covariance matrix. At last singular value decomposition is done on the covariance matrix. As a results we will get singular values and singular vectors. Here singular values tell's us how much of the variance is explained by corresponding principal components. Now, principal components are calculated by multiplying spectra with singular numbers.

Spectral indices are ratios, sums or different arithmetic combinations of spectral bands. They return single map, which can correlate with some properties of the images object. For example, in the remote sensing of vegetation indices such as normalized difference vegetation index (NDVI) or modified chlorophyll absorption in reflectance index (MCARI). NDVI is calculated as

$$\frac{NIR - RED}{NIR + RED}, \tag{4}$$

where NIR is some near infrared band (between 0.7 to 1 μm) and RED is band from red region of the visible light (between 0.65 to 0.7 μm). MCARI is defined as

$$\frac{(R_{850} - R_{730} - 0.2 \times (R_{850} - R_{570}))}{R_{730}}, \tag{5}$$

where R_i denotes to reflectance on wavelength i. Implemented indices library includes almost 300 different spectral indices.

The development focus was mainly on workflow and processes that produces magic behind the curtains: the least amount of effort is three clicks from start to whole spectral cube and one click more to start analyzing. What CubeView offers, is an effective and new way to capture cubes, show analysis results and produce quick demos to the researchers, corporate decision makers and even to consumers. It brings new innovations, wraps algorithms and scientific research in to easily approached and partly productized form.

Spectral Imaging Laboratory will release mentioned libraries and first standalone versions of CubeView during the spring 2019.

5. RESULTS

A measurement was done to test a hyperspectral imager and the new CubeView software. The selected imaging target was plastic leaves of a non-organic plant and one real leaf from a healthy plant. Without close examination both types of leaves appear to be organic to naked eye. The target was illuminated by a broad band light source to ensure that whole wavelength range of measurement is covered. The parameters of PFPI that was used in HSI for this measurement are summarized in table 2. The figure 6 shows the resulting PCA and abundance maps, as well as endmembers, which correlate to certain unique material features of the target. The measured wavelength range was $450 - 850$ nm with camera set to analog gain of 10x and exposure to 120 ms. The figure 7 shows the output of spectral angle mapper. It can be seen in figure 7, that with threshold value of 0.1 the real plant leaf is highlighted, indicating a strong similarities in spectra with the real plant. Finally, the figure 8 shows a comparison of regular RGB-composite image and a NDVI image. It can be seen, that NDVI is much higher for real plant as it is expected due to chlorophyll absorption.
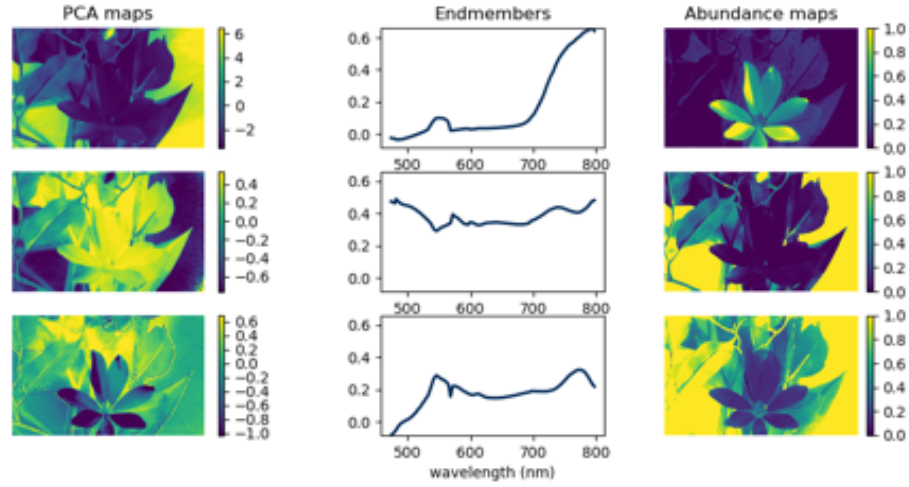

Figure 6: Results of principal component analysis (PCA) (left), and vertex component analysis (VCA) (middle and right).
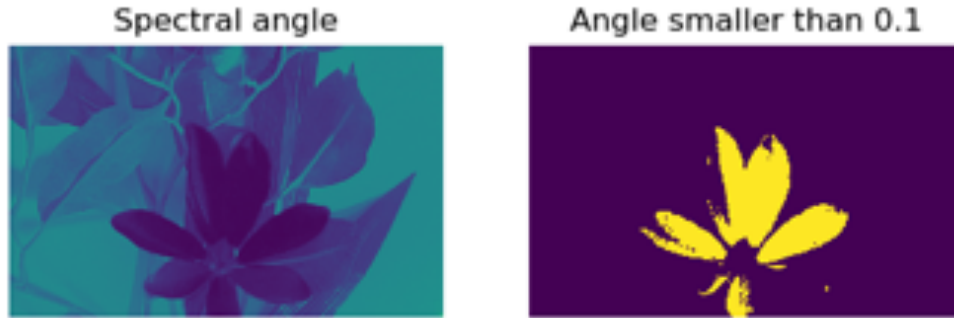

Figure 7: Spectral angle as compared to a pixel spectra from the real plant (left) and thresholded spectral angle (right).
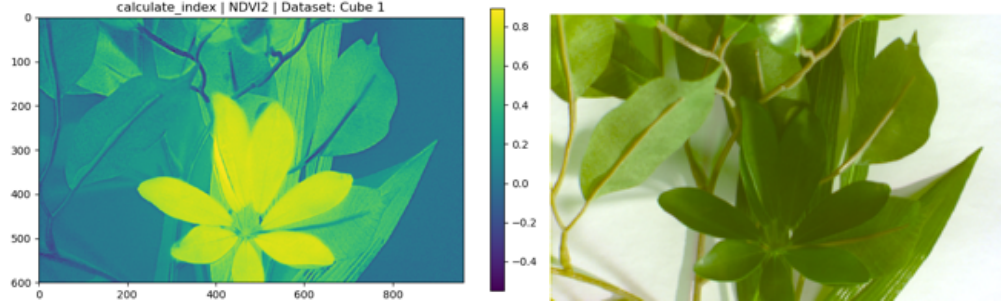
Figure 8: NDVI-index (left) and RGB-composite of three selected bands (right).

6. SUMMARY AND CONCLUSIONS

This paper presented a way to mitigate two common problems that are associated with hyperspectral imagery. The first is the unavailability of flexible and affordable imager hardware platform. The other is the raw spectral data, that are typically unusable for most of applications without an analysis algorithm. It was shown that it is possible to develop compact, low cost, portable, hyperspectral imager, that supports both MFPI and PFPI technologies. As result, the hardware platform can be used in wider range of applications, further reducing costs and increasing availability of hyperspectral imaging. In addition to the hardware, the newly developed software tool was tested with a hyperspectral camera system and it was shown, that it is possible to use PCA analysis to find and highlight the unique spectral features within raw data cube. Therefore, the user is given quick access to more visually understandable spectral information.

REFERENCES

[1] Näsilä, A., Trops, R., Stuns, I., Havia, T., Saari, H., Guo, B., Ojanen, H. J., Akujärvi, A., and Rissanen, A., "Hand-held mems hyperspectral imager for vnir mobile applications," *Proc.SPIE* **10545**, 10545 – 10545 – 9 (2018).

[2] Rissanen, A., Guo, B., Saari, H., Näsilä, A., Mannila, R., Akujärvi, A., and Ojanen, H., "Vtt's fabry-perot interferometer technologies for hyperspectral imaging and mobile sensing applications," *Proc.SPIE* **10116**, 10116 – 10116 – 12 (2017).

[3] Rissanen, A., Saari, H., Rainio, K., Stuns, I., Viherkanto, K., Holmlund, C., Näkki, I., and Ojanen, H., "Mems fpi-based smartphone hyperspectral imager," *Proc.SPIE* **9855**, 9855 – 9855 – 16 (2016).

[4] Eskelinen, M. A. and Hämäläinen, J., "Fabry-perot imaging in python." https://github.com/silmae/fpipy (2018). [Online; accessed 19-Dec-2018].

[5] Annala, L., Eskelinen, M., Hämäläinen, J., Riihinen, A., and Pölönen, I., "Practical approach for hyperspectral image processing in python," in [*International Archives of the Photogrammetry, Remote Sensing and Spatial Information Sciences*], **42**(3), International Society for Photogrammetry and Remote Sensing (2018).

[6] Nascimento, J. M. and Dias, J. M., "Vertex component analysis: A fast algorithm to unmix hyperspectral data," *IEEE transactions on Geoscience and Remote Sensing* **43**(4), 898–910 (2005).

[7] Chang, C.-I. and Plaza, A., "A fast iterative algorithm for implementation of pixel purity index," *IEEE Geoscience and Remote Sensing Letters* **3**(1), 63–67 (2006).

[8] Lawson, C. L. and Hanson, R. J., [*Solving least squares problems*], vol. 15, Siam (1995).

[9] Yuhas, R. H., Goetz, A. F., and Boardman, J. W., "Discrimination among semi-arid landscape endmembers using the spectral angle mapper (sam) algorithm," in [*JPL, Summaries of the Third Annual JPL Airborne Geoscience Workshop*], **1**, 147–149 (1992).